Spectroscopy 16 (2002) 127–138
IOS Press

The use of the time-resolved X-ray solution scattering for studies of globular proteins

Kunihiro Kuwajima [a,*], Munehito Arai [a,b], Tomonao Inobe [a], Kazuki Ito [c], Masaharu Nakao [a], Kosuke Maki [a], Kiyoto Kamagata [a], Hiroshi Kihara [d] and Yoshiyuki Amemiya [e]
[a] *Department of Physics, School of Science, University of Tokyo, Bunkyo-ku, Tokyo 113-0033, Japan*
[b] *Institute of Molecular Cell Biology, NIAIST, Tsukuba, Ibaraki 305-8566, Japan*
[c] *Institute of Materials Science, University of Tsukuba, Ibaraki 305-8572, Japan*
[d] *Department of Physics, Kansai Medical University, Hirakata, Osaka 573-1136, Japan*
[e] *Depatment of Advanced Materials Science, Graduate School of Frontier Science, University of Tokyo, Bunkyo-ku, Tokyo 113-8656, Japan*

Abstract. In order to improve the low signal-to-noise ratio of the time-resolved small-angle X-ray scattering, we have used a two-dimensional X-ray detector with a beryllium-windowed X-ray image intensifier and a charge-coupled device as an image sensor, and applied this to studies on (1) the kinetic folding reaction of α-lactalbumin, which accumulates the molten globule-like intermediate at an early stage of refolding and (2) the cooperative conformational transition of *Escherichia coli* chaperonin GroEL induced by ATP, which occurs in an allosteric manner between the close and open conformational states. In the α-lactalbumin reaction, we have firmly established the equivalence between the kinetic intermediate and the equilibrium molten globule state, and obtained further information about dehydration from the highly hydrated folding intermediate during a late stage of refolding. In the chaperonin study, we have successfully observed the kinetics of the allosteric transition of GroEL that occurs with a rate constant of about 3–4 s^{-1} at 5°C. The combination of the time-resolved X-ray scattering with other spectroscopic techniques such as circular dichroism and intrinsic fluorescence is thus very effective in understanding the conformational transitions of proteins and protein complexes.

1. Introduction

Small-angle X-ray scattering (SAXS) is a powerful technique for studying directly changes in the size and shape of a protein molecule and a protein complex in solution [1,2], and should be complimentary in the acquired structural information to other spectroscopic techniques such as circular dichroism, fluorescence, and vibrational spectroscopy. In combination with a stopped-flow technique, we have previously used the time-resolved SAXS to investigate kinetic folding of globular proteins [3,4]. However, the low signal-to-noise (S/N) ratio of the time-resolved SAXS measurement has hampered us from obtaining the desired information about the molecular size and shape within a millisecond time region of the reactions.

In the present study, we have overcome the above problem by using a two-dimensional (2D) detector with a beryllium-windowed X-ray image intensifier and a charge-coupled device (CCD) as an image sensor. The sensitivity of the 2D detector is higher than a one-dimensional position-sensitive proportional counter, and the use of the 2D detector has improved the S/N ratio dramatically by circular averaging the SAXS patterns that have circular symmetry [5–7].

We have studied (1) the kinetic refolding reaction of α-lactalbumin, which accumulates the molten globule-like intermediate at an early stage of folding, and (2) the cooperative conformational transition

*Corresponding author. Tel.: +81 3 5841 4128; Fax: +81 3 5841 4128; E-mail: kuwajima@phys.s.u-tokyo.ac.jp.

of *Escherichia coli* chaperonin GroEL induced by ATP, which occurs in an allosteric manner between the close and open conformational states. In the α-lactalbumin reaction, the molten globule intermediate has previously been characterized by various spectroscopic techniques, including circular dichroism and hydrogen-exchange labeling NMR spectroscopy, and has been shown to have native-like secondary structure but lack the specific tertiary packing of amino acid side chains [8,9]. By the stopped-flow SAXS in the present study, we have firmly established the equivalence between the kinetic intermediate and the equilibrium molten globule state, and obtained further information about dehydration from the highly hydrated folding intermediate during a late stage of refolding. In the chaperonin study, we have successfully observed the kinetics of the allosteric transition of GroEL that occurs with a rate constant of about 3–4 s^{-1} at 5°C, and this corresponds to the second phase of the ATP-induced kinetics of a tryptophan mutant of GroEL previously observed by stopped-flow fluorescence studies [10,11]. Therefore, in both cases, the results obtained by the time-resolved SAXS give us new insights into the conformational transitions of proteins, and the technique is very effective when combined with the other spectroscopic techniques such as circular dichroism, fluorescence, and vibrational spectroscopies.

2. Materials and methods

2.1. Materials

Bovine α-lactalbumin was purified from crudely purified powder purchased from Sigma (St. Louis, MO) as described previously [12]. An expression plasmid for a tryptophan-inserted mutant (Y485W) of GroEL, in which tryptophan was substituted for Tyr458, was constructed from the plasmid pEL-WT, which encoded wild-type GroEL, with a QuikChange site-directed mutagenesis kit (Stratagene). Purification of GroEL and the Y485W mutant was carried out as described previously [13–15]. Guanidine hydrochloride (GdnHCl) was specially prepared reagent grade for biochemical use from Nacalai Tesque, Inc. (Kyoto, Japan). ATP was purchased from Sigma (St. Louis, MO). Other chemicals were guaranteed reagent grade. The concentration of the proteins was determined spectrophotometrically using an extinction coefficient, $E^{1\%}_{1\,\mathrm{cm}} = 20.1$, 2.1, and 3.05 for α-lactalbumin, GroEL, and the Y485W mutant, respectively, at 280 nm. The concentration of GdnHCl was determined from the refractive index at 589 nm [16]. Solutions were filtered through membrane filters (pore size 0.45 μm) before measurements. All solutions for α-lactalbumin contained 50 mM sodium cacodylate (pH 7.0), 50 mM NaCl, and 1 mM $CaCl_2$, except for the equilibrium molten globule state (10 mM HCl (pH 2.0)). Solutions for the chaperonin contained 50 mM Tris-HCl (pH 7.5), 10 mM $MgCl_2$, 100 mM KCl, and the indicated amount of ATP.

2.2. SAXS measurements

SAXS measurements were performed at beamline 15A of the Photon Factory at the High Energy Accelerator Research Organization, Tsukuba, Japan as described previously [7,17]. Briefly, the sample solution in a sapphire- and a mica-windowed cell for stopped-flow and static measurements, respectively, had a 1-mm path length, and was irradiated with a monochromatic X-ray beam (1.5 Å). The intensity of the beam at the sample position was $1 \times 10^{10} \sim 2.4 \times 10^{10}$ photons/s. The CCD-based X-ray detector is composed of the beryllium-windowed X-ray image intensifier (Hamamatsu, V5445P-MOD), an optical lens coupling, and an interline transfer-mode CCD (Hamamatsu, C7300) as an image sensor [5]. Data were collected in a range of scattering vector, Q, from 0.015 to 0.2 $Å^{-1}$, where Q is given by $Q = 4\pi \sin\theta/\lambda$ (λ, wavelength; and 2θ, scattering angle).

Stopped-flow SAXS measurements were carried out using a stopped-flow apparatus constructed by Unisoku, Inc., Osaka, Japan, as described previously [4,7]. The dead time of the mixing was 7 ($\pm$2) ms.

2.3. SAXS analysis

When the CCD-based X-ray detector is applied to the SAXS experiments, it is necessary to make corrections to the data, because the CCD-based X-ray detector has its own intrinsic distortion of images, non-uniformity of response, and contrast reduction of the X-ray image intensifier. The procedures for these corrections were described elsewhere (Ito et al., manuscript in preparation) [18,19] and carried out accordingly.

The radius of gyration $R_{\rm g}$ of the scatterer and the zero-angle intensity $I(0)$ were obtained based on the Guinier approximation,

$$\ln I(Q) = \ln I(0) - \left(R_{\rm g}^2 Q^2\right)/3 \tag{1}$$

at small-angle regions, where $\ln I(Q)$ is linearly dependent on Q^2 [1,2].

The time-dependent change in the $R_{\rm g}^2$, $I(0)$ or integral intensity $I_{\rm int}$ value was fitted to a single-exponential function,

$$A(t) = A(\infty) + \Delta A \exp(-k \cdot t) + at, \tag{2}$$

where $A(t)$ and $A(\infty)$ are $R_{\rm g}^2$, $I(0)$ or $I_{\rm int}$ at time t and at infinite time, respectively, ΔA is the change in the amplitude, k is the rate constant of the reaction, and the last term at was introduced for correction, if required, for beam damage of the protein.

2.4. Stopped-flow fluorescence measurement

The fluorescence kinetics of the Y498W mutant of GroEL were measured in an SX.18MV stopped-flow spectrometer (Applied Photophysics; Leatherhead, UK) by monitoring the change in fluorescence above 320 nm when excited at 295 nm (5.1°C). The optical path length was 0.2 cm, and the dead time of the apparatus was approximately 4 ms. The time-dependent change in the fluorescence intensity $F(t)$ was fitted to the following equation by the nonlinear least-squares method

$$F(t) = F(\infty) + \sum_i \Delta F_i \exp(-k_i \cdot t), \tag{3}$$

where $F(\infty)$ is the fluorescence intensity at infinite time, and ΔF_i and k_i are the amplitude and the rate constant, respectively, of the ith phase.

3. Results and discussion

3.1. Refolding of α-lactalbumin

α-Lactalbumin, a monomeric globular protein with a molecular weight of 14,200, is one of the best-studied proteins in protein folding. It forms the molten globule state at equilibrium that has a native-like secondary structure, a hydrophobic core exposed to solvent, and a compact size with a radius of

Fig. 1. Schematic representation of bovine α-lactalbumin (PDB code: 1HFZ). A black ball shows one calcium ion bound to the protein molecule. Four disulfide bonds are shown by ball-and-stick. In the molten globule state, the α-domain consisting of three α-helices and a 3_{10} helix is more organized than the β-domain that consists of a three-stranded β-sheet and a 3_{10} helix, being less organized. The figure was prepared with the program MOLMOL [26].

gyration, $R_{\rm g}$, only 10% larger than that of the native state but lacks most of the specific side-chain packing interactions (Fig. 1) [8,9]. The results of the kinetic refolding experiments using various spectroscopic techniques, including circular dichroism, vibrational, aromatic absorption, fluorescence, and pulsed hydrogen-exchange labeling NMR spectroscopy, have shown that the protein accumulates a kinetic folding intermediate within the dead time of the stopped-flow measurements, and the characteristics of the intermediate are coincident with those of the equilibrium molten globule state [9]. However, because of the lack of kinetic methods to monitor the size and overall shape of a protein molecule with a time resolution of milliseconds, the compactness of the kinetic folding intermediate has not yet been clarified. Thus, here we measured the equilibrium and kinetics of folding-unfolding reactions of α-lactalbumin by the SAXS technique using the 2D CCD-based X-ray detector.

To determine the conditions for the kinetic experiments, we first measured the equilibrium unfolding transition of α-lactalbumin by SAXS (Fig. 2). The $R_{\rm g}$ of a protein molecule was obtained from Guinier approximation of a scattering curve at small-angle regions by Eq. (1) (see Materials and methods), and the transition curve was monitored by $R_{\rm g}^2$, because the observed $R_{\rm g}^2$ value is known to be represented by linear combination of the $R_{\rm g}^2$ values of the native, intermediate, and/or unfolded states [1,2]. The results show that the protein is in the native state at less than 2 M GdnHCl, while it is in the unfolded state above 3.5 M GdnHCl.

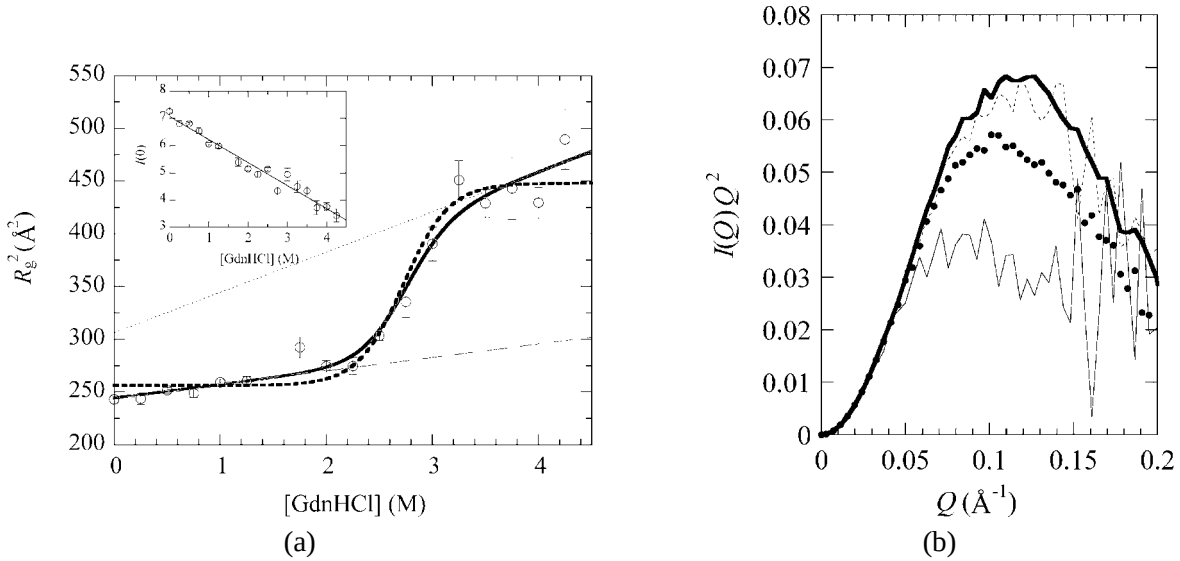

Fig. 2. (a) The GdnHCl-induced equilibrium unfolding transition of α-lactalbumin monitored by R_g^2. The thick lines are the theoretical transition curves assuming a two-state transition. In the calculation of the thick continuous line, the R_g^2 values in the native and fully unfolded states, $(R_g^2)_N$ and $(R_g^2)_U$, respectively, are assumed to linearly depend on GdnHCl concentration. The thin dotted and dashed lines are the baselines for the unfolded and the native states, respectively. In the calculation of the thick broken line, constant values for $(R_g^2)_N$ and $(R_g^2)_U$ are assumed. The $(R_g^2)_N$ and $(R_g^2)_U$ values thus obtained are 256 ± 6 Å^2 and 448 ± 8 Å^2, respectively. The free energy of unfolding ΔG_{NU}, the cooperativity index m, and the transition midpoint, c_M, are 7.0 ($\pm$0.4) kcal mol^{-1}, 2.6 ($\pm$0.1) kcal mol^{-1} M^{-1}, and 2.7 ($\pm$0.2) M, respectively [7]. The inset shows the GdnHCl concentration dependence of $I(0)$, which is fitted linearly. The $I(0)$ values were corrected for absorption of X-ray by GdnHCl. Errors are standard errors in fitting of Guinier plots. (b) The Kratky plots of α-lactalbumin at 0 M (thick continuous line), 0.75 M (thin broken line), and 4 M GdnHCl (thin continuous line). Filled circles show the Kratky plot of the equilibrium molten globule state at pH 2. The scattering intensities of each plot are normalized with respective $I(0)$ values.

Figure 3 shows a kinetic refolding curve measured by the R_g values during the refolding reaction induced by a concentration jump of GdnHCl from 4 M to 0.77 M. Changes in the R_g^2 values were fitted to a single-exponential function by Eq. (2) (see Materials and methods), and the rate constant of the refolding reaction thus obtained was 0.49 ($\pm$0.07) s^{-1}, which is in agreement with the rate measured by other spectroscopic techniques. The R_g value after the refolding reaction was 15.5 ($\pm$0.1) Å, and the R_g value at zero time of refolding obtained by extrapolation of the fitting curve to zero time was 17.5 ($\pm$0.2) Å. Because this protein forms the transient folding intermediate within the dead time of the stopped-flow measurement, the folding intermediate has the R_g of 17.5 ($\pm$0.2) Å, which is in good agreement with the known R_g value of the equilibrium molten globule state (Table 1) [20].

Figure 4 shows SAXS patterns for transient states at different times during the refolding (10–20 ms, 10–110 ms, and 10–960 ms after the initiation of refolding), for the native state after the refolding reaction has completed (8–11 s), and for the equilibrium molten globule state at pH 2, all represented by the Kratky plot [1,2]. Because the refolding reaction has a time constant of 2.0 ($\pm$0.3) s, the scattering pattern averaged within 10–20 ms of refolding must correspond to the pattern for the transient folding intermediate. Figure 4 thus shows that the scattering pattern of the transient folding intermediate is coincident with that of the equilibrium molten globule state. Therefore, the present data of the R_g values and the profiles of the Kratky plots clearly show that the transient folding intermediate has the same molecular size and shape as the equilibrium molten globule state, and when combining these results with

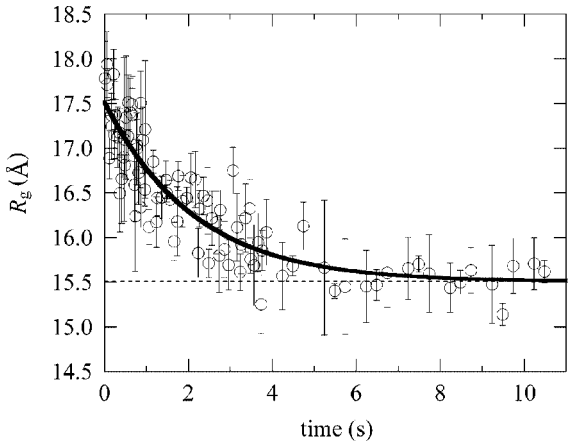

Fig. 3. Time-dependent changes in the R_g during the refolding reaction of α-lactalbumin. Time-dependent changes in the R_g^2 were fitted to a single exponential function, and the fitting curve of the R_g thus obtained is shown in the figure (thick continuous line). The rate constant of the reaction was 0.49 ($\pm$0.07) s^{-1}. The dotted line shows the R_g value after the refolding is completed. Errors are standard error in fitting of Guinier plots.

Table 1
Radius of gyrations of α-lactalbumin in different states

State	R_g (Å)
Equilibrium	
Native	15.5
Molten globule	17.5
Fully unfolded	21.0
Kinetic burst-phase intermediate	17.5

the previous results by other spectroscopic techniques, we can firmly conclude that the transient folding intermediate of α-lactalbumin is equivalent to the equilibrium molten globule state.

The Guinier analysis of the present SAXS data has shown that not only the R_g but also the $I(0)$ value varies during the kinetic refolding of α-lactalbumin, and Fig. 5 shows these changes in the $I(0)$. The time dependence of $I(0)$ fits in with a single-exponential function with a rate constant of 0.65 ($\pm$0.14) s^{-1}, which is similar to the refolding rate constant of the protein. The $I(0)$ value at zero time of refolding obtained by extrapolation of the fitting curve is 1.10 ($\pm$0.01) times larger than the $I(0)$ of the native state. The $I(0)$ of the SAXS is generally given by

$$I(0) = (\Delta\rho v)^2 = [(\rho_1 - \rho_0)v]^2, \tag{4}$$

where $\Delta\rho$ is the difference in the electron density between the protein (ρ_1) and the solvent water (ρ_0), and v is the volume of the protein [1,2]. Because α-lactalbumin does not show any aggregation under the present condition, the larger $I(0)$ for the transient folding intermediate is probably due to the presence of more hydrated waters in the intermediate than in the native state. The hydrated water on the protein surface has been shown to have 1.1 times larger electron density than bulk water [21], and the equilibrium molten globule state is known to have more hydrated water molecules than the native state [8,9]. Therefore, if we assume $\rho_0 = 0.33$ $e^-/Å^3$, $\rho_1 = 0.45$ $e^-/Å^3$ for the native protein [2], and the R_g values for the intermediate and the native state shown in Table 1, Eq. (4) leads to an estimate of about 140 excess

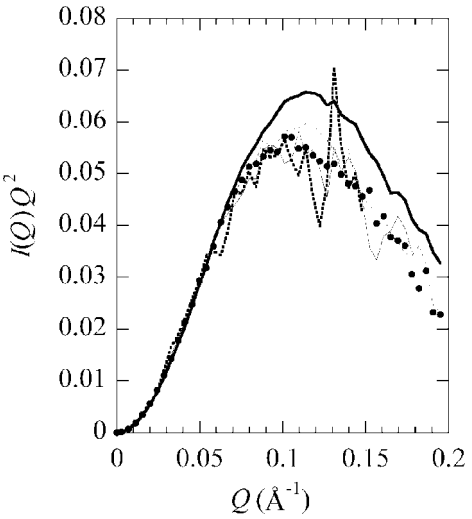

Fig. 4. The Kratky plots of α-lactalbumin averaged between 10 and 20 ms after the initiation of refolding (thick dotted line), between 10 and 110 ms (thin continuous line), between 10 and 960 ms (thin broken line), and between 8 and 11 sec (thick continuous line). Filled circles show the Kratky plot of the equilibrium molten globule state at pH 2. The scattering intensities of each plot are normalized with respective $I(0)$ values.

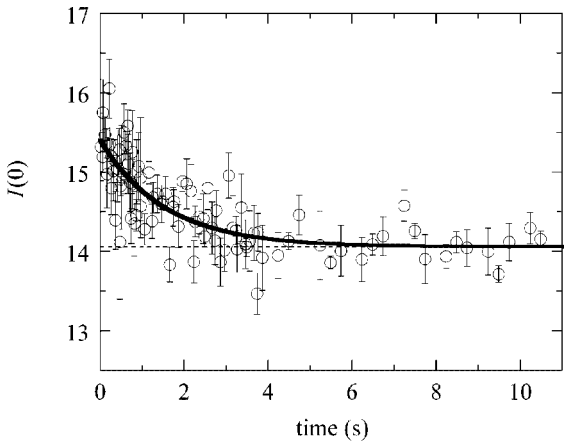

Fig. 5. Time-dependent changes in $I(0)$ during the refolding of α-lactalbumin. The thick continuous line is a fitting curve assuming a single-exponential function. The dotted line shows the $I(0)$ value after the refolding is completed. Errors are standard errors in fitting of Guinier plots.

hydrated water molecules present in the intermediate. The decrease in $I(0)$ in Fig. 5 may thus be caused by dehydration of the excess hydrated waters in the intermediate during the refolding.

3.2. The allosteric transition of GroEL

The chaperonin GroEL, a tetradecameric protein complex composed of two rings stacked back-to-back on each other with each ring consisting of seven identical subunit of 57 kDa, is one of the best characterized molecular chaperones [22]. The X-ray crystallographic structure of GroEL has revealed that each subunit of GroEL consists of three domains, an equatorial domain that contains a nucleotide

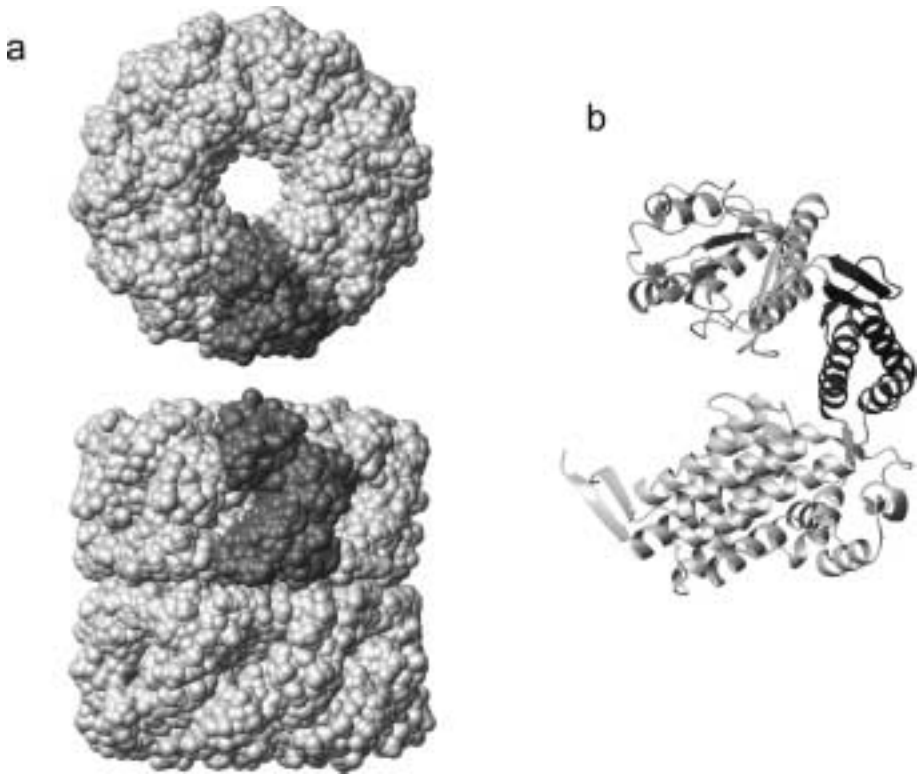

Fig. 6. The X-ray crystallographic structure of GroEL. (a) The 14-mer structure: the top view (top) and the side view (bottom). (b) The structure of a single subunit. The apical (light grey), intermediate (dark grey) and equatorial (white) domains are shown.

binding site as well as most of the interaction sites between monomers and most of the contact regions between the heptameric rings, an apical domain that contains a binding site for a target protein, and an intermediate domain that connects the equatorial and apical domains (Fig. 6) [23].

The full functional activity of GroEL requires the co-chaperonin GroES and the nucleotide ATP, and the allosteric transitions of GroEL induced by ATP are important for regulating the affinity of GroEL for its target proteins [22,24]. The nested allosteric model proposed by Yifrach and Horovitz assumes two levels of allostery, one within each ring and the second between the rings [25]. In the first level, the allosteric transition occurs from the T to the R state in accordance with the Monod–Wyman–Changeux model with positive cooperativity with respect to ATP, where T and R denotes tense and relaxed states, respectively, for a single-ring part of the GroEL complex. In the second level of allostery, GroEL undergoes sequential Koshland–Némethy–Filmer-type transitions from the TT via the TR to the RR state with negative cooperativity between the rings. However, these allosteric transitions have so far been investigated by the ATPase assay of GroEL or fluorescence spectroscopy of tryptophan mutants of GroEL [10,11,14, 25], and there is no direct structural data of the real-time allosteric transitions in solution. Therefore, here we have applied the SAXS technique with the 2D detector to investigating the allosteric transitions of GroEL.

Figure 7 shows the SAXS patterns of GroEL at 0 M, 85 μM and 3 mM ATP at 25°C. At 0 M ATP, GroEL is in the TT state. At 85 μM ATP, the SAXS pattern was measured during a period between 0.5 and 2.0 s after mixing of ATP and GroEL by the use of the stopped-flow apparatus, where the amount of the ATP hydrolyzed must be less than 6 μM. Therefore, the concentration of the un-hydrolyzed ATP

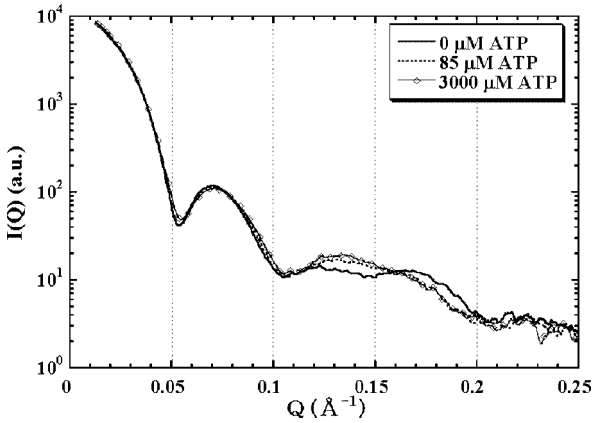

Fig. 7. SAXS patterns of GroEL at 0 M (continuous line), 85 μM (dotted line) and 3 mM ATP (continuous line with open circles) at 25°C. The scattering intensity $I(Q)$ is shown as a function of Q.

was larger than 79 μM, and the GroEL was mostly in the TR state, because the TT to TR transition is fast enough as compared with a delay time (0.5 s) for the SAXS measurement, and the ATP hydrolysis is slow enough as compared with the time of the SAXS measurement; the apparent rate constant of the TT to TR transition is an order of 10 s^{-1} at 80 μM ATP and 25°C (unpublished data). At 3 mM ATP, ATP hydrolysis was in the steady state, and GroEL was in the so-called RR state.

The SAXS patterns of the three allosteric states of GroEL thus obtained are different from each other, reflecting the allosteric conformational changes of the GroEL particle. However, compared with clearly discernible differences between the TT and the TR states in a range of the scattering vector Q from 0.12 to 0.2 Å^{-1}, the differences between the TR and the so-called RR state are very minor (Fig. 7). This indicates that the conformational change from TR to the so-called RR is not equivalent to the change from TT to TR and that the RR may be fairly similar in structure to the TR state.

We next studied the kinetics of the TT to TR transition of GroEL by stopped-flow SAXS measurements. We monitored the transition induced by mixing GroEL and ATP with the final concentrations of 3.8 μM (GroEL) and 85 μM (ATP) at 4.8°C. The low temperature was used to increase the S/N ratio by decelerating the kinetics. We used the integral scattering intensity, $I_{\text{int}} = \int I(Q)\,\mathrm{d}Q$, in a region of Q from 0.06 to 0.08 Å^{-1} to follow the kinetics of the structural change. This further increased the S/N ratio, and the resultant kinetic trace is shown in Fig. 8(a). The kinetics monitored by I_{int} in a different Q region from 0.09 to 0.15 Å^{-1} was found to coincide with that of Fig. 8(a) (data not shown). When the time course of I_{int} was fitted to a single exponential function, the apparent rate obtained was 3.38 ($\pm$0.39) s^{-1}. The apparent rate constant measured by I_{int} was found to increase with ATP concentration, and it was 7.0 ($\pm$1.5) s^{-1} at 124 μM ATP. A small increase in I_{int} after 2 s seen in Fig. 8(a) was due to beam damage of GroEL by X-ray, the intensity of which was more than two times in the kinetic experiments than in the static experiments. The beam damage became more noticeable with increasing time, but the overall scattering pattern was not significantly affected in the time range shown in Fig. 8(a).

Figure 8(b) shows the transient scattering curves of GroEL measured at early and late stages (10–310 ms and 1.5–3 s, respectively, after mixing of GroEL and ATP) of the ATP-induced kinetics. These transient SAXS curves are the results of data accumulation of about 400 shots of the stopped-flow mixing. The averaged scattering curve between 10 and 310 ms shows characteristic of the TT state, while the averaged scattering curve between 1.5 and 3.0 s is coincident with that in the TR state (Fig. 7), affording clear evidence that the kinetics observed by I_{int} represents the ATP-induced TT to TR transition of GroEL.

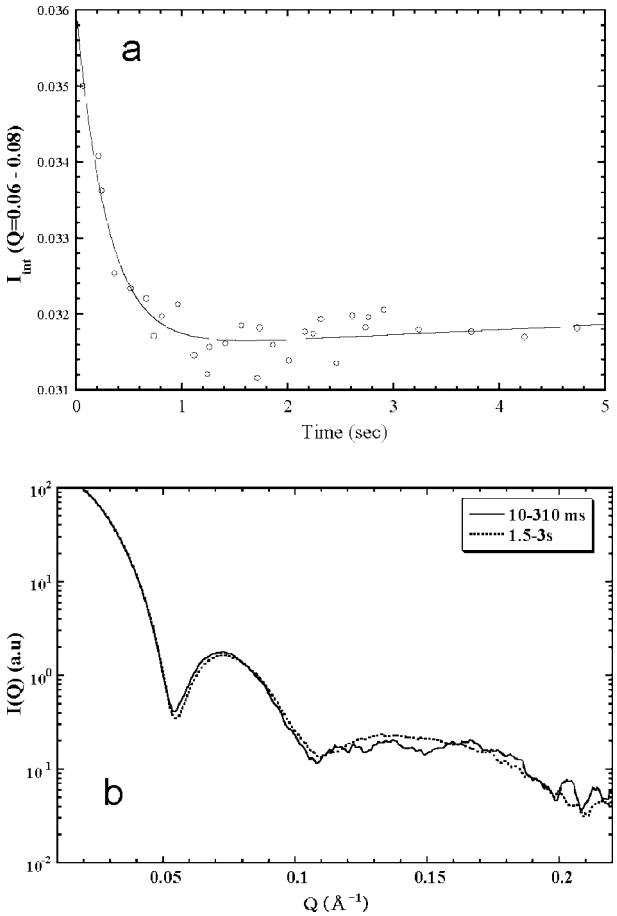

Fig. 8. (a) A kinetic curve of the ATP-induced structural change of GroEL at 4.8°C monitored by $I_{\rm int}$. The integral region of Q employed was from 0.06 to 0.08 Å^{-1}. The structural change was initiated by a mixing with ATP (final concentrations of 3.8 μM and 85 μM for GroEL and ATP, respectively). The continuous line shows a theoretical kinetic progress curve assuming single exponential. (b) The SAXS patterns were averaged between 10 ms and 310 ms (continuous line) and between 1.5 sec and 3 sec (dotted line).

We finally studied the kinetics of the ATP-induced structural transition of GroEL by stopped-flow fluorescence measurements using a tryptophan-inserted mutant of GroEL (Y485W), so as to correlate the SAXS-detected kinetics with the fluorescence-detected ones. Figure 9 shows fluorescence-monitored kinetics of the Y485W mutant (0.5 μM) when mixed with ATP (85 μM) at 5.1°C. The kinetics are composed of four phases: the first phase occurring within 0.15 s and accompanied by an increase in the fluorescence intensity, the second and third phases with rate constants of 4.5 and 0.88 s^{-1}, respectively, and both accompanied by a decrease in the fluorescence intensity, and the fourth phase that shows an increase in the fluorescence with the rate constant of 0.013 s^{-1}. As compared with the kinetics measured by SAXS, the second phase corresponds to the kinetic process observed by $I_{\rm int}$ that has the rate constant of 3.38 ($\pm$0.39) s^{-1}. The results thus indicate that the second phase observed by the fluorescence kinetics represents the conformational transition of GroEL from the TT to the TR state. We also observed similar four-phase kinetics by fluorescence at 25.0°C but with increased rate constants (data not shown), which were coincident with the kinetics previously reported by Cliff et al. [11].

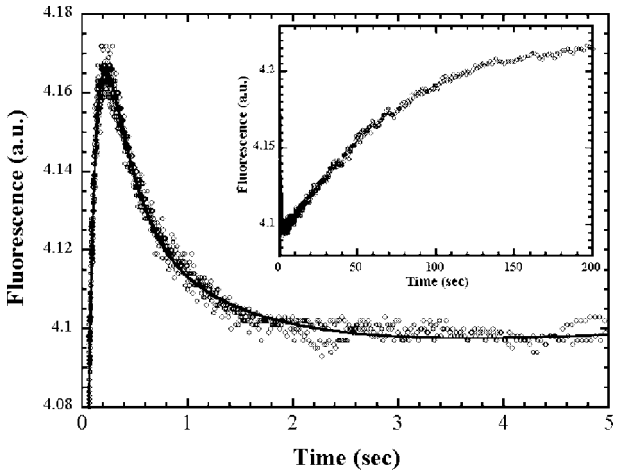

Fig. 9. Kinetics of the ATP-induced fluorescence change of tryptophan-inserted mutant of GroEL (Y485W). The Y485W mutant (0.5 μM) was mixed with ATP (85 μM) at 5.1°C. Time-dependent changes of fluorescence were fitted to four exponential functions, and the fitting curve of the fluorescence thus obtained is shown in the figure (thick continuous line). The first phase occurred within 0.15 s and accompanied by an increase in the fluorescence intensity, the second and third phases were with rate constants of 4.5 and 0.88 s^{-1}, respectively, and both accompanied by a decrease in the fluorescence intensity, and the fourth phase showed an increase in the fluorescence with a rate constant of 0.013 s^{-1}.

4. Conclusions

We have applied the SAXS with the 2D CCD-based detector using the beryllium-windowed X-ray image intensifier to the folding study of α-lactalbumin and the study of the allosteric transition of the chaperonin GroEL complex. As a result, we have firmly established the equivalence of the transient folding intermediate formed in the burst-phase of refolding and the molten globule state of the protein, and we have successfully identified the TT to TR allosteric transition step in the complex kinetics of GroEL induced by ATP. The equilibrium and kinetic SAXS technique is thus very effective for the studies of globular proteins, especially when we use the technique in combination with other spectroscopic techniques such as circular dichroism, fluorescence, and vibrational spectroscopies.

Acknowledgements

We thank Professor Katsuzo Wakabayashi for giving us an opportunity to use the CCD-based X-ray detector coupled with the beryllium-windowed X-ray image intensifier and Dr. Hironari Kamikubo for technical assistance with the SAXS measurements. This study was performed under approval of the Photon Factory (Proposal No. 97P006, 98P036, 99G343, and 2000G325) and was supported by Grants-in-Aid for Scientific Research from the Ministry of Education, Science and Culture of Japan.

References

[1] O. Glatter and O. Kratky, Small angle X-ray scattering, in: *Small Angle X-ray Scattering*, London, Academic Press, 1982.
[2] S. Doniach, Changes in biomolecular conformation seen by small angle X-ray scattering, *Chemical Reviews* **101** (2001), 1763–1778.

[3] G.V. Semisotnov, H. Kihara, N.V. Kotova, K. Kimura, Y. Amemiya, K. Wakabayashi, I.N. Serdyuk, A.A. Timchenko, K. Chiba, K. Nikaido, T. Ikura and K. Kuwajima, Protein globularization during folding. A study by synchrotron small-angle X-ray scattering, *J. Mol. Biol.* **262** (1996), 559–574.
[4] M. Arai, T. Ikura, G.V. Semisotnov, H. Kihara, Y. Amemiya and K. Kuwajima, Kinetic refolding of β-lactoglobulin. Studies by synchrotron X-ray scattering, and circular dichroism, absorption and fluorescence spectroscopy, *J. Mol. Biol.* **275** (1998), 149–162.
[5] Y. Amemiya, K. Ito, N. Yagi, Y. Asano, K. Wakabayashi, T. Ueki and T. Endo, Large-aperture TV detector with a beryllium-windowed image intensifier for X-ray diffraction, *Rev. Sci. Instrum.* **66** (1995), 2290–2294.
[6] M. Arai, K. Ito, K. Maki, T. Ikura, T. Inobe, H. Kihara, Y. Amemiya and K. Kuwajima, Structural analysis of protein folding intermediates by solution X-ray scattering, in: *Old and New Views of Protein Folding*, K. Kuwajima and M. Arai, eds, Elsevier, Amsterdam, 1999, pp. 31–40.
[7] M. Arai, K. Ito, T. Inobe, M. Nakao, K. Maki, K. Kamagata, H. Kihara, Y. Amemiya and K. Kuwajima, Fast compaction of α-lactalbumin during folding studied by stopped-flow X-ray scattering, *J. Mol. Biol.* **321** (2002), 121–132.
[8] O.B. Ptitsyn, Molten globule and protein folding, *Adv. Protein Chem.* **47** (1995), 83–229.
[9] M. Arai and K. Kuwajima, The role of the molten globule state in protein folding, *Adv. Protein Chem.* **53** (2000), 209–282.
[10] O. Yifrach and A. Horovitz, Transient kinetic analysis of adenosine 5′-triphosphate binding-induced conformational changes in the allosteric chaperonin GroEL, *Biochemistry* **37** (1998), 7083–7088.
[11] M.J. Cliff, N.M. Kad, N. Hay, P.A. Lund, M.R. Webb, S.G. Burston and A.R. Clarke, A kinetic analysis of the nucleotide-induced allosteric transitions of GroEL, *J. Mol. Biol.* **293** (1999), 667–684.
[12] K. Kuwajima, Y. Hiraoka, M. Ikeguchi and S. Sugai, Comparison of the transient folding intermediates in lysozyme and α-lactalbumin, *Biochemistry* **24** (1985), 874–881.
[13] T. Makio, M. Arai and K. Kuwajima, Chaperonin-affected refolding of α-lactalbumin: Effects of nucleotides and the co-chaperonin GroES, *J. Mol. Biol.* **293** (1999), 125–137.
[14] T. Inobe, T. Makio, E. Takasu-Ishikawa, T.P. Terada and K. Kuwajima, Nucleotide binding to the chaperonin GroEL: non-cooperative binding of ATP analogs and ADP, and cooperative effect of ATP, *Biochim. Biophys. Acta* **1545** (2001), 160–173.
[15] T. Makio, E. Takasu-Ishikawa and K. Kuwajima, Nucleotide-induced transition of GroEL from the high-affinity to the low-affinity state for a target protein: Effects of ATP and ADP on the GroEL-affected refolding of α-lactalbumin, *J. Mol. Biol.* **312** (2001), 555–567.
[16] C.N. Pace, Determination and analysis of urea and guanidine hydrochloride denaturation curves, *Methods Enzymol.* **131** (1986), 266–280.
[17] Y. Amemiya, K. Wakabayashi, T. Hamanaka, T. Wakabayashi, T. Matsushima and H. Hashizume, Design of a small-angle X-ray diffractometer using synchrotron radiation at the phton factory, *Nucl. Instrum. Meth. Phys. Res.* **208** (1983), 471–477.
[18] K. Ito and Y. Amemiya, CCD-based X-ray detectors, *J. Jpn. Soc. Synchrotron Rad. Res.* **13** (2000), 372–381.
[19] K. Ito, H. Kamikubo, M. Arai, K. Kuwajima, Y. Amemiya and T. Endo, Calibration method for contrast reduction problem in the X-ray image intensifier, *Photon Factory Activity Report* **18** (2001), 275–275.
[20] M. Kataoka, K. Kuwajima, F. Tokunaga and Y. Goto, Structural characterization of the molten globule of α-lactalbumin by solution X-ray scattering, *Protein Sci.* **6** (1997), 422–430.
[21] D.I. Svergun, S. Richard, M.H. Koch, Z. Sayers, S. Kuprin and G. Zaccai, Protein hydration in solution: experimental observation by X-ray and neutron scattering, *Proc. Natl. Acad. Sci. USA* **95** (1998), 2267–2272.
[22] W.A. Fenton and A.L. Horwich, GroEL-mediated protein folding, *Protein Sci.* **6** (1997), 743–760.
[23] K. Braig, P.D. Adams and A.T. Bruenger, Conformational variability in the refined structure of the chaperonin GroEL at 2.8 Å resolution, *Nature Struct. Biol.* **2** (1995), 1083–1094.
[24] Z.H. Xu, A.L. Horwich and P.B. Sigler, The crystal structure of the asymmetric GroEL-GroES-(ADP)7 chaperonin complex, *Nature* **388** (1997), 741–750.
[25] O. Yifrach and A. Horovitz, Nested cooperativity in the ATPase activity of the oligomeric chaperonin GroEL, *Biochemistry* **34** (1995), 5303–5308.
[26] R. Koradi, M. Billeter and K. Wüthrich, MOLMOL: a program for display and analysis of macromolecular structures, *J. Mol. Graphics* **14** (1996), 51–53.